

# First evidence for poloidal asymmetries of radial ion energy transport by ion temperature measurements in the scrape-off layer of Tore Supra

M. Kočan and J. P. Gunn

CEA, IRFM, F-13108 Saint-Paul-lez-Durance, France

## 1. Introduction

The intermittent expulsion of plasma filaments, or “blobs”, from the last closed flux surface (LCFS) is believed to be responsible for a large fraction of the radial particle transport in the scrape-off layer (SOL) [1]. Blobs appear to be initiated by a ballooning-type instability in the unfavourable curvature region on the low field side (LFS). As they propagate outward, they also expand along the magnetic field lines, driving parallel flows [2]. When the plasma contact point is on the inboard limiters, the blobs propagate freely out to the wall leading to a broad SOL with nearly flat density profiles. On the other hand, it was demonstrated that outboard limiters suppress the radial transport, leading to a very thin SOL [3].

The first evidence for poloidal asymmetry of the radial ion and electron energy transport in the SOL, similar to that of the particle transport [3], is reported. Implications for ITER start-up phase are discussed. Correlation of the asymmetries of SOL ion ( $T_i$ ) and electron ( $T_e$ ) temperatures on each side of the probe with changes of the parallel Mach number  $M_{||}$ , important for the Mach probe theory, is addressed.

## 2. Experimental results

Tore Supra ohmic discharges with the plasma contact point either on the inboard bumper limiters (referred to as “inboard discharges”) or on the outboard antenna protection limiters (“outboard discharges”) are studied. The database comprises 22 inboard (including 4 detached) and 4 outboard measurements (including 1 detached), Fig. 1 and Tab. 1. The working gas is deuterium. Both  $I_p$  and  $B_t$  are oriented clockwise looking from the top of the torus. SOL  $T_i$ ,  $T_e$  and the parallel ion saturation current density  $j_{sat}$  have been measured simultaneously from both directions along the magnetic field lines by a bidirectional retarding field analyzer (RFA) [4]. The RFA is located at  $R = 2.53$  m and moves vertically, Fig. 1. Electron density and the heat flux density are calculated as  $n_e = j_{sat} / [0.35e^{1.5} \sqrt{(T_i + T_e) / m_i}]$

[5] (with  $j_{sat} = \sqrt{j_{sat}^{HFS} \cdot j_{sat}^{LFS}}$ , HFS/LFS indicating respectively the analyzer facing the high

parameter	inboard	outboard
$a$ [m]	0.60 – 0.68	0.47 – 0.65
$R$ [m]	2.18 – 2.26	2.39 – 2.52
$\langle n_e \rangle$ [ $10^{19} \text{ m}^{-3}$ ]	0.9 – 4.7	1.4 – 5
$I_p$ [MA]	0.4 – 1.2	0.3 – 0.7
$q_a$	3.4 – 9.2	3.5 – 8.5
$B_t$ [T]	3.2 – 4.1	3.5 – 3.7
$f_{rad}$	0.3 – ~1	0.4 – 0.8
$P_{in}$ [MW]	0.3 – 1.2	0.3 – 0.7

Tab. 1. Macroscopic parameters of the database discharges. From top to bottom: minor radius, major radius, volume averaged density, plasma current, safety factor at  $a$ , toroidal magnetic field, radiated power fraction and ohmic input power.

field side and the low field side, Fig. 6) and  $q_{||} = \gamma T_e j_{sat}$ , respectively. The total heat transmission coefficient  $\gamma$  is calculated from Eq.(25.46) in [6].  $T_i$  is calculated as  $(T_i^{HFS} + T_i^{LFS}) / 2$  [7]. A model for the HFS/LFS asymmetry of  $T_e$  is not yet available and  $T_e$  is also calculated as  $(T_e^{HFS} + T_e^{LFS}) / 2$ .

Fig. 2 shows the radial profiles measured in selected inboard and outboard discharges. The former is characterized by a factor of 4 longer e-folding lengths compared to latter.  $T_i > T_e$  is consistent with the observations reported from other tokamaks (Fig. 7 in [8]).

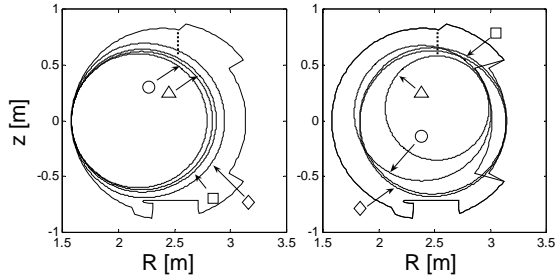


Fig. 1. Poloidal cross sections included in the database. Left: inboard contact point. Right: outboard contact point. Vertical dotted line indicates the RFA location.

Note that for the outboard discharges the LCFS at the RFA location calculated by the EFIT poloidal field reconstruction (referred to as “EFIT LCFS”) was found to be shifted inward by up to  $\sim 2$  cm compared to the LCFS given by the Taylor extrapolation of the magnetic flux measurements (referred to as a “Taylor LCFS”). This leads to a large uncertainty in the LCFS values, Fig. 2. It is not yet clear which magnetic reconstruction is more reliable. However, for deep reciprocations performed by other Langmuir probes in the outboard discharges a sharp increase of  $T_e$  and  $j_{sat}$  (possibly related to the transition between the SOL and the confined region) coincides with the Taylor LCFS. Therefore, in what follows Taylor LCFS is considered. For the inboard discharges EFIT and Taylor LCFS overlap within a few millimeters.

Fig. 3 shows the e-folding lengths of  $T_i$ ,  $T_e$ ,  $n_e$  and  $q_{||}$  for all database discharges, plotted against the volume averaged density. The e-folding lengths are calculated from the data measured between the LCFS and the next most inner limiter. For a given configuration several macroscopic parameters are varied and their influence on the e-folding lengths thus cannot be decoupled. In general, however, the outboard discharges have substantially shorter e-folding lengths compared to the inboard discharges. For the database discharges  $T_i = 5 - 65$  eV,  $T_e = 5 - 30$  eV and  $T_i/T_e = 1 - 5$  at the LCFS. The lowest  $T_i$ ,  $T_e$  and  $T_i/T_e$  is measured in detached plasmas.

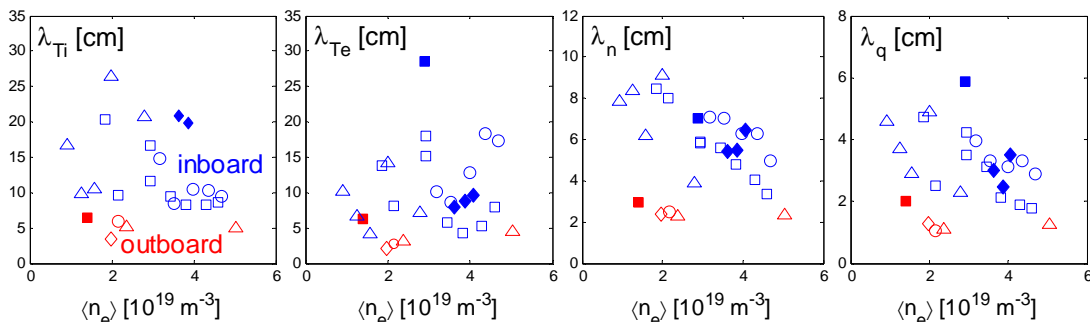


Fig. 3. The e-folding lengths of  $T_i$ ,  $T_e$ ,  $n_e$  and  $q_{||}$  plotted against the volume-averaged plasma density. Inboard / outboard indicate the contact point. Symbols correspond to poloidal cross sections from Fig. 1. Full symbols: detached discharges.  $\lambda_{T_i}$  for two detached discharges is almost infinite and does not appear on graph.

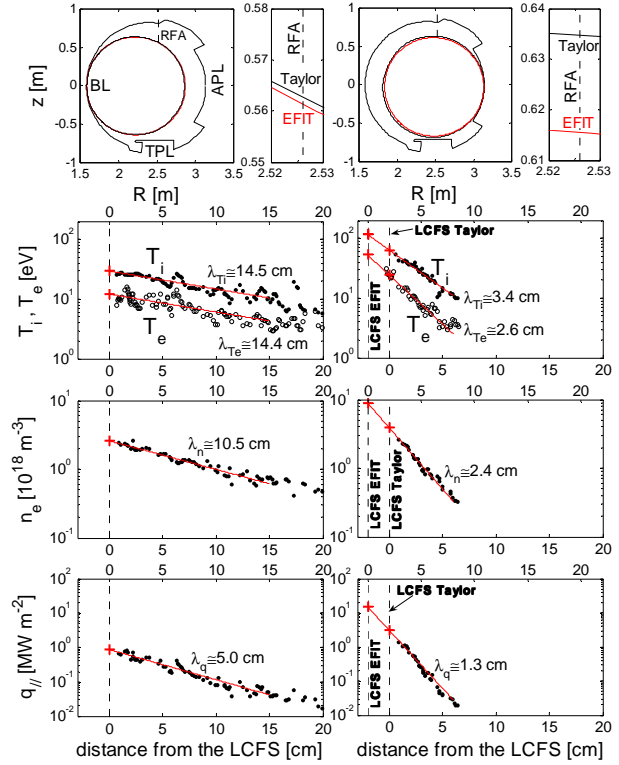


Fig. 2. SOL profiles measured by RFA. Left: inboard discharge. Right: outboard discharge. From top to bottom: LCFS with the magnified region of the RFA location (BL: bumper limiter, APL: antenna protection limiter, TPL: toroidal pump limiter), ion and electron temperatures, electron density, parallel heat flux density with e-folding lengths. Two LCFS reconstructions (Taylor, EFIT) are shown.

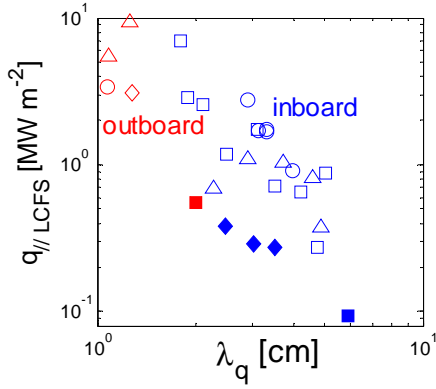


Fig. 4. Heat flux density at the LCFS plotted against the SOL heat flux density e-folding length. Full symbols: detached discharges.

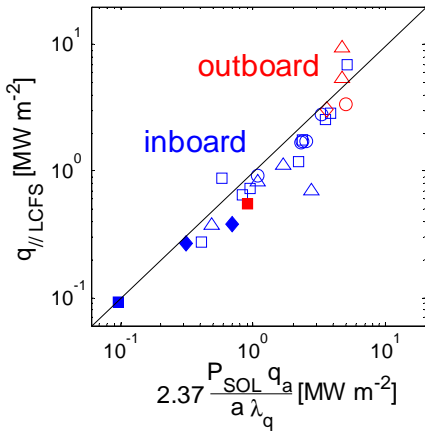


Fig. 5. Parallel heat flux density at the LCFS plotted against the physics-based scaling.

$q_{||LCFS}$  is obtained for the EFIT LCFS) as well as the extrapolation of the measured  $q_{||}$  towards the LCFS over the distance comparable to  $\lambda_q$ . Another important point to consider is that our measurements were performed in circular plasmas so that the scaling might not be valid for the elongated ITER start-up plasma. It is important to note that if  $T_i$  were not measured, the usual assumption of  $T_i = T_e$  would underestimate  $q_{||LCFS}$  up to a factor of  $\sim 2.3$  for the discharges studied here.

The asymmetries of ion and electron temperatures measured by each side of the RFA were studied in a discharge #42403 during which the plasma contact point was steadily displaced upward along the outboard limiter, Fig. 6. Such displacement is known to be associated with the reversal of the parallel plasma flow [3]. According to kinetic calculations from [7], the flow reversal should be associated with similar changes of the effective  $T_i$  measured by each side of the RFA. Fig. 6 shows the radial profiles of  $T_i$ ,  $T_e$  and  $j_{sat}$  measured by each side of the RFA. Also shown is the parallel Mach number calculated as  $M_{||} \equiv 0.4 \ln(j_{sat}^{LFS} / j_{sat}^{HFS})$  [6].  $T_i^{LFS} / T_i^{HFS}$  clearly changes with the change of  $M_{||}$  but, in contrary to the theory [7], it does not reverse completely like  $j_{sat}$ . This suggests that some of the assumptions in the kinetic modeling of the behavior of the pre-sheath surrounding the RFA [7] might not be valid. Interestingly, a similar asymmetry is also measured for  $T_e$ . A model for the asymmetry of  $T_e$  is not yet available. It should be noted that one of the assumptions of the fluid Mach probe

As shown in Figs. 2-4, the poloidal asymmetry in the particle and energy transport makes the e-folding length of  $q_{||}$ ,  $\lambda_q$ , strongly dependent on the plasma contact point. In addition, as seen from Fig. 4  $q_{||}$  at the LCFS  $q_{||LCFS} \propto \lambda_q^{-1}$  and is thus highest in the outboard discharges. This has an important consequence e.g. for the ITER start-up phase for which two outboard modular limiters are currently envisaged [9].  $q_{||LCFS} \propto \lambda_q^{-1}$  has a physical background in the conservation of the power in the SOL  $P_{SOL} \approx 2\pi R \int q_{\theta} dr \approx 2\pi R q_{\theta LCFS} \lambda_q \approx$

$R q_{||LCFS} \lambda_q (B_{\theta} / B_{tot}) \approx q_{||LCFS} \lambda_q a / q_a$  (where  $q_a$  is the safety factor at the minor radius  $a$ ), so that  $q_{||LCFS} \approx P_{SOL} q_a / (a \lambda_q)$ . Fig. 5 shows that such physics-based scaling reproduces well  $q_{||LCFS}$  for both contact points and over a large range of parameters.  $P_{SOL} q_a / (a \lambda_q)$  in Fig. 5 is multiplied by a constant  $C = 2.37$  (for  $P_{SOL} = P_{in}(1 - f_{rad})$  in MW,  $a$  in meters and  $\lambda_q$  in centimeters) obtained from the linear least-square fit. The predictive capability of the scaling of  $q_{||LCFS}$  to ITER plasma is obviously very limited as the database (of the outboard discharges in particular) is statistically insignificant. In addition, for the outboard discharges a large error on  $q_{||LCFS}$  should be anticipated because of the uncertainty of the LCFS position (a factor of 3 – 4 higher

theory [5,10] is that the parallel electron velocity distribution is Maxwellian, in which case the same  $T_e$  would be measured by each side of the RFA.

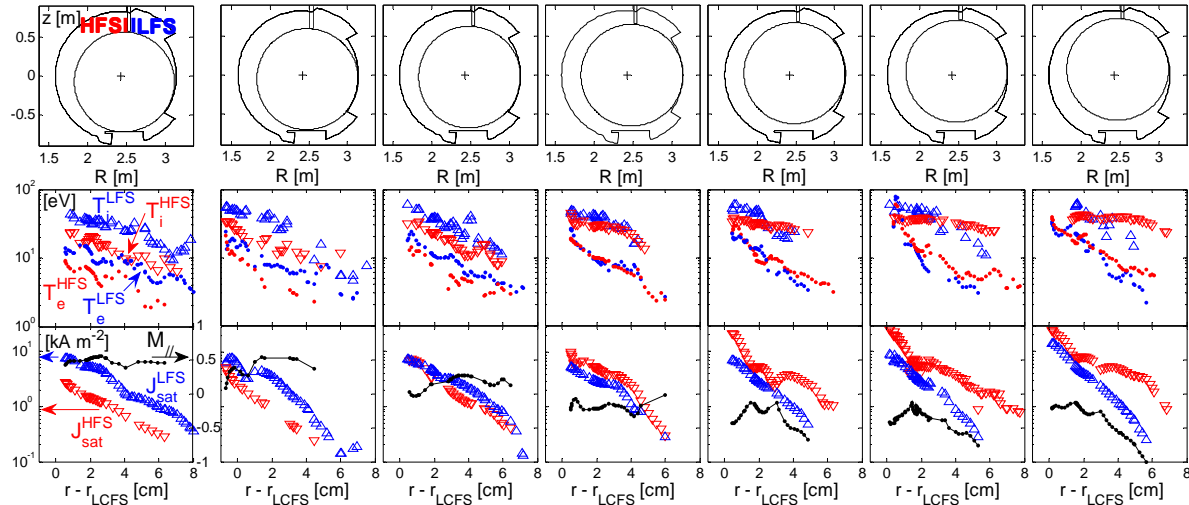


Fig. 6. Radial profiles of  $T_i$ ,  $T_e$ ,  $j_{sat}$  and  $M_{||}$  measured in seven RFA reciprocations in the discharge with steadily displaced outboard contact point. HFS / LFS indicate the side of the RFA. For  $M_{||} > 0$  the flow is directed towards the LFS analyzer.

### 3. Conclusions

New measurements carried out with the RFA in Tore Supra have demonstrated, although on a very limited database, that the poloidal asymmetry of the radial ion and electron energy transport in the SOL is similar to that of the particle transport [3]. These results are particularly important for the ITER start-up phase which is currently envisaged on the outboard modular limiters and for which the modelled peak heat loads on the limiters were found to be considerably close to the engineering limit [9]. The physics-based scaling for the parallel heat flux density at the LCFS  $q_{||LCFS} \propto P_{SOL} \lambda_q^{-1}$  was found to agree with measurements. It implies that the outboard start-up is least advantageous with regards to power handling as it may be characterized by large, localized heat loads. We do not attempt to scale the heat flux densities found in Tore Supra to ITER. We suggest that alternative start-up scenarios (e.g. the start-up on the inboard side, eventually in a detached regime) should be evaluated. Systematic measurements of the type presented here, as well as in elongated plasmas, are necessary to enhance the predictive capability of the scaling to ITER.

### Acknowledgement

This work, supported by the European Communities under the contract of Association between EURATOM and CEA, was carried out within the framework of the European Fusion Development Agreement. The views and opinions expressed herein do not necessarily reflect those of the European Commission. The authors acknowledge helpful discussions with Dr. François Saint-Laurent about the magnetic surface reconstruction methods and excellent technical assistance of Jean-Yves Pascal.

### References

- [1] V. Naulin, J. Nucl. Mater. **363-365** (2007) 24, [2] N. Asakura, J. Nucl. Mater. **363-365** (2007) 41, [3] J. P. Gunn *et al.*, J. Nucl. Mater. **363-365** (2007) 484, [4] M. Kočan *et al.*, Rev. Sci. Instrum. **79** (2008) 073502, [5] I. H. Hutchinson, Phys. Fluids **30** (1987) 3777, [6] P. C. Stangeby, *The Plasma Boundary in Magnetic Fusion Devices* (Bristol: Institute of Physics Publishing, 2000) [7] F. Valsaque *et al.*, Phys. Plasmas **9** (2002) 1806, [8] M. Kočan *et al.*, Plasma Phys. Control. Fusion **50** (2008) 125009, [9] M. Kobayashi *et al.*, Nucl. Fusion **47** (2007) 61, [10] J. P. Gunn and V. Fuchs, Phys. Plasmas **14** (2007) 032501.